NEW CARBON MATERIALS
Volume 28, Issue 5,Oct 2013
Online English edition of the Chinese language journal

Available online at www.sciencedirect.com
ScienceDirect

Cite this article as: New Carbon Materials, 2013, 28(5):327–335.

RESEARCH PAPER

pH-dependent size，surface chemistry and electrochemical properties of graphene oxide

WU Hui[1], LU Wei[1,2,*], SHAO Jiao-jing[1], ZHANG Chen[1], WU Ming-bo[3], LI Bao-hua[2], YANG Quan-hong[1,2,*]

[1]School of Chemical Engineering and Technology, Tianjin University, Tianjin 300072, China;
[2]Engineering Laboratory for Functionalized Carbon Materials, Graduate School at Shenzhen, Tsinghua University, Shenzhen 518055, China;
[3]State Key Laboratory of Heavy Oil Processing, China University of Petroleum, Qingdao 266580, China

Abstract: The size and surface chemistry of graphene oxide (GO) dispersed in an aqueous solution are tuned by adjusting the pH value of the parent GO hydrosol. This method is based on the protonation of the carboxyl groups on GO nanosheets (GONs) in an acidic environment and the partial removal of oxygen-containing functional groups in strong basic conditions. GONs with a high electrochemical activity can be obtained by tuning the pH-dependent sheet sizes and the fraction of functional groups. It is found that the functional groups of a GON are more crucial in providing a high electrochemical activity than are the plane edges, and the size of a GON is also a key factor to influence the chemical activity. GONs with smaller sheet sizes but similar functional groups show a weaker electrochemical activity than those with larger sizes. In addition, GONs possess a high activity towards H_2O_2 detection and hence are promising for use as an electrode of biosensors.

Key Words: Graphene oxide; pH value; Surface chemistry; Electrochemical activity

1 Introduction

Graphene oxide (GO), an exfoliation product of graphite oxide, can be viewed as the most important chemical derivative of graphene because of the existence of rich functional groups[1,2]. These groups endow GO with good processability and higher chemical activity than graphene in solution, since the existing sp^3-hybridized carbons related to hydroxyl and epoxy groups distribute on graphitic carbon regions and those related to carboxyl groups attach on the edges[3]. Thus, GO is widely used as a starting material to assemble specific graphene-based materials by wet chemistry methods, such as functionalized graphenes, graphene oxide membranes and graphene-based macroforms[4-11]. Therefore, the properties of these GO derivatives are largely influenced by the characters of GO, such as the sheet size, C/O ratio[12-14]. Recent reports have proven that the properties of GO directly affect the chemical activity and the microstructure of the obtained graphene derivatives[4, 9, 15-20]. Regrettably, the nature of GO is still not very clear due to the complexity of sheet size and functional groups, which hinder the precise structure and property control of these GO derivatives[2].Thus, it is necessary to understand and find an efficient way to tune the chemical properties of GO, especially its features in aqueous solution, for a controllable assembly of graphene-based materials.

The functional groups attached on the graphene framework have a high chemical activity and can specifically react with some organic molecules and biomaterials, making GO an active material in biosensors[21-25]. Furthermore, the rich functional groups also bring a specific catalytic activity and a high electron transfer rate in organic reaction[26]. The functional groups and sheet size are proved to be the two key factors that make GO sensitive to environment[27]. GO nanosheets (GONs) of a certain size show different dispersing abilities in the aqueous solution at various pH values, which can be used to sieve the GONs with specific sizes[28,29]. Especially, deoxygenation reaction will occur when GONs come across the strong basic condition, which would influence their chemical activities[30].

In this paper, the size and surface chemistry of the GONs well dispersed in aqueous solutions are finely controlled by tuning the pH value of the parent GO hydrosol, and its corresponding electrochemical activities are investigated in detail. The results demonstrate that both functional groups and sheet size are the two key factors influencing the electrochemical activities of GONs. Besides, the GONs are revealed to be the active materials for H_2O_2 detection and their sensing performance can also be tuned by changing the above two factors.

2 Experimental

2.1 Preparation of GO hydrosol with different pH values

Received date: 9 May 2013; **Revised date:** 23 September 2013
***Corresponding author.** E-mail: qhyangcn@tju.edu.cn, lv.wei@sz.tsinghua.edu.cn
Copyright©2013, Institute of Coal Chemistry, Chinese Academy of Sciences. Published by Elsevier Limited. All rights reserved.
DOI: 10.1016/S1872-5805(13)60085-2

Graphite oxide was firstly prepared according to the modified Hummers method [15]. 80 mg graphite oxide was added in 80 mL deionized water and subjected to a strong sonication (200 W) for 2 h (JY92-N, China). Then a certain amount of HCl or KOH solution was introduced into the obtained GO hydrosol to adjust their pH values to 3, 5, 7, 9, 11 and 12, and then centrifugation (~3 800 r/min, 5 min) was employed to remove the unstable GONs (very little deposit after centrifugation). The obtained hydrosols were denoted as GO-X, where X represented the pH value of the hydrosol. It is noted that the obtained GO-3 shows a high transparency and a color of brown, while the hydrosols turn into black when pH values are increased to 11 and 12.

2.2 Preparation of GO modified electrodes

The glassy carbon (GC, diameter: 2 mm) electrode surface was firstly polished with alumina slurries with particle size of 1.5 μm, 0.7 μm and 50 nm and sonicated for 5 min twice in deionized water and ethanol. Then, 6 μL GO-X hydrosol was dropped on GC electrode and dried at room temperature. After that, 2 μL Nafion solution (5%) was finally casted and used as a binder to hold the GO-X on the electrode surface stably.

2.3 Sample characterization

Microscopic morphology of the GONs was observed using a transmission electron microscope (TEM, JEOL JEM-2100F, Japan). The size distribution and zeta potential of GONs were carried out on Zetasizer Nano ZS (Malvern, England) at 25 °C. Transmittance of GO-X hydrosol was measured by an ultraviolet-visible spectrophotometer (UV-1102, China) after the hydrosol was diluted 40 times. Surface chemistry analysis for the GO-X was conducted by using X-ray photoelectron spectroscopy (XPS, Escalab 250, Al *K*α, USA).

2.4 Electrochemistry measurements

The electrochemical performance of GO-X modified GC electrodes was measured by an electrochemistry workstation (CHI660C). A GO-X modified GC electrode was employed as the working electrode. Saturated calomel electrode and platinum foil were used as the reference electrode and counter electrodes, respectively. Cyclic voltammetry (CV) measurement was conducted to characterize the electrochemical reaction occurring on the working electrode surface in $K_3Fe(CN)_6$ electrolyte solution, in which KCl (0.05 mol/L) was used as supporting electrolyte. The electrochemical activity towards H_2O_2 detection was conducted in 0.01 mol/L phosphate buffer solution (PBS) containing 0.05 mol/L KCl (pH value = 7.4) using CV and chronoamperometry. All experiments were carried out at room temperature. Note that the concentration of the GO only affects the current density of the electrode while the peak separation, which reflects the activity of the electrode, will not be affected.

3 Results and discussion

3.1 Characterization of GONs with different pH values

After an ultra-sonication process, graphite oxide is fully exfoliated into few layers, as shown in the TEM image in Fig. 1a. The obtained GO hydrosols at different pH values, which are subjected to a sonication, followed by a centrifugation, show a high stability in both acidic and basic environment (pH value ranges from 3 to 12) and no aggregations and precipitations can be observed after being stored for several months (as shown in the inset of Fig. 1d). We also used a high-precision nanoparticle size analyzer to reveal the statistical size distributions of GONs in different GO hydrosols. As shown in Fig. 1b, we can see that small GONs with the size in the range of 200-500 nm are favorable to the acidic or basic environment, while the larger GONs, whose sizes distribute at about 500 nm-1.5 μm, prefer to exist in the neutral and alkalescent conditions. The sheet size is considered to be mainly influenced by carboxyl groups on the GON edge. Therefore, ionization of these groups is the dominant factor in acidic suspension, while the situation became complicated in the basic environment since the neutralization reaction occurred between the acidic carboxyl groups and the alkali added. Consequently, both ionization and reduction of carboxyl groups should be considered in basic environment. A reasonable explanation is given as follows. Generally, the edge-to-area ratio of GON increases with the decrease of its lateral dimension. Thus, smaller GONs should have a higher solubility than larger counterparts because of higher densities of ionized $–COO^-$ groups. In acidic environment, with the decrease of the pH value, the ionized $–COO^-$ groups are gradually protonated, leading to the deposition of larger GONs. And in basic environment, the –COOH groups will be partly removed due to the counteract reaction, which also causes a precipitation of the larger GONs from suspension. The above results suggest a new route for precisely controlling the size of GONs in solution.

From the zeta potentials shown in Fig. 1 c, we can see that the zeta potentials drop with decreasing of the pH values of GO hydrosols, indicating that the edge carboxyl groups are protonated at the acidic condition. It should be noted that the aggregation occurs if the pH value is lower than 2 due to the highly protonation of the $–COO^-$ groups. In the alkaline environment, although a lot of functional groups have been removed under higher pH value, the zeta potential is more negative. This is caused by the repulsion between deprotonated carboxyl groups of GONs. Fig. 1d shows that the transmittance of GO hydrosol continuously decreases with the increase of pH value, and the color of the hydrosol changes from brown to black gradually. Combining the above discussions, it is considered that this color transformation should be affected by the sizes and surface chemistry. After an addition of KOH, GONs are deoxygenated and reduced to some extent. When the pH value increases to 11, the deoxygenation degree is very high inducing a color transformation

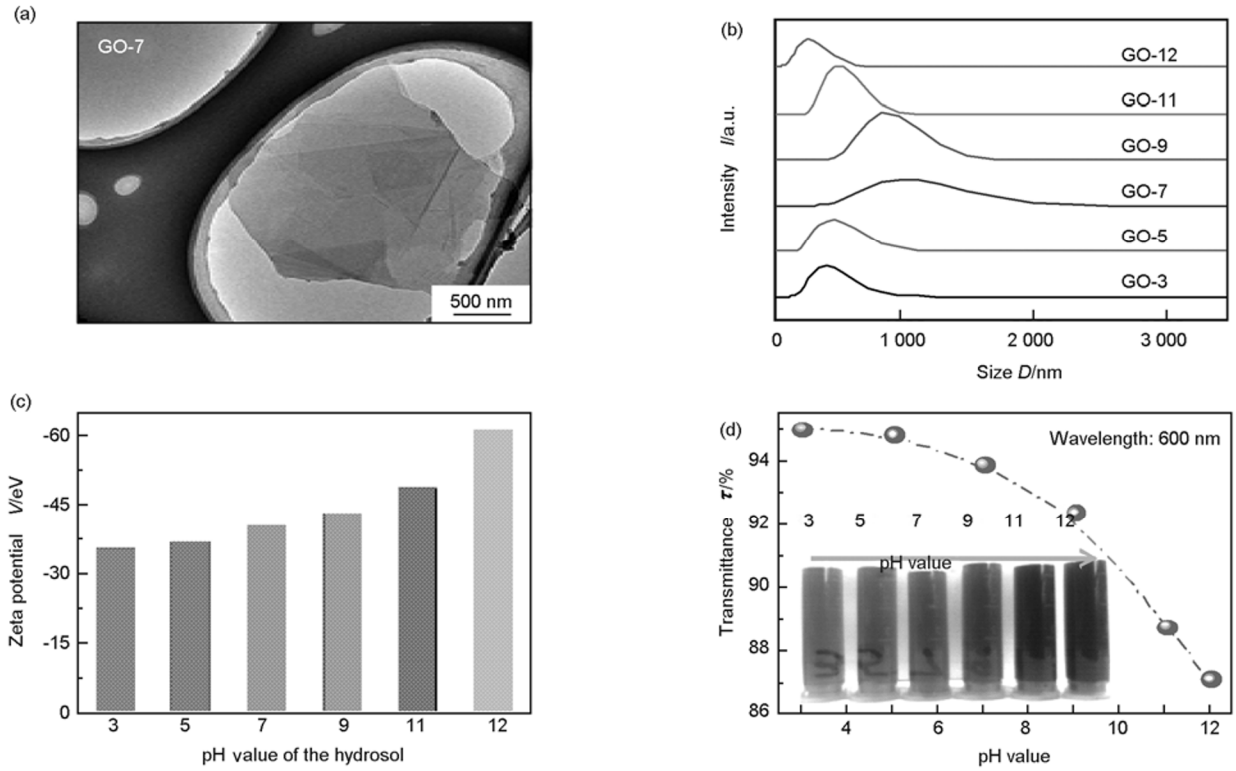

Fig. 1 pH-dependent size sieving effects of GONs and optical properties of GO hydrosols. (a) TEM image of GONs dispersed in the hydrosol with a pH value of 7; (b) Size distributions of GONs; (c) Zeta potential and (d) optical transmittance of the GO hydrosol (diluted 40 times) with different pH values at a wavelength of 600 nm, and the inset of (d) shows the digital photo of the hydrosols.

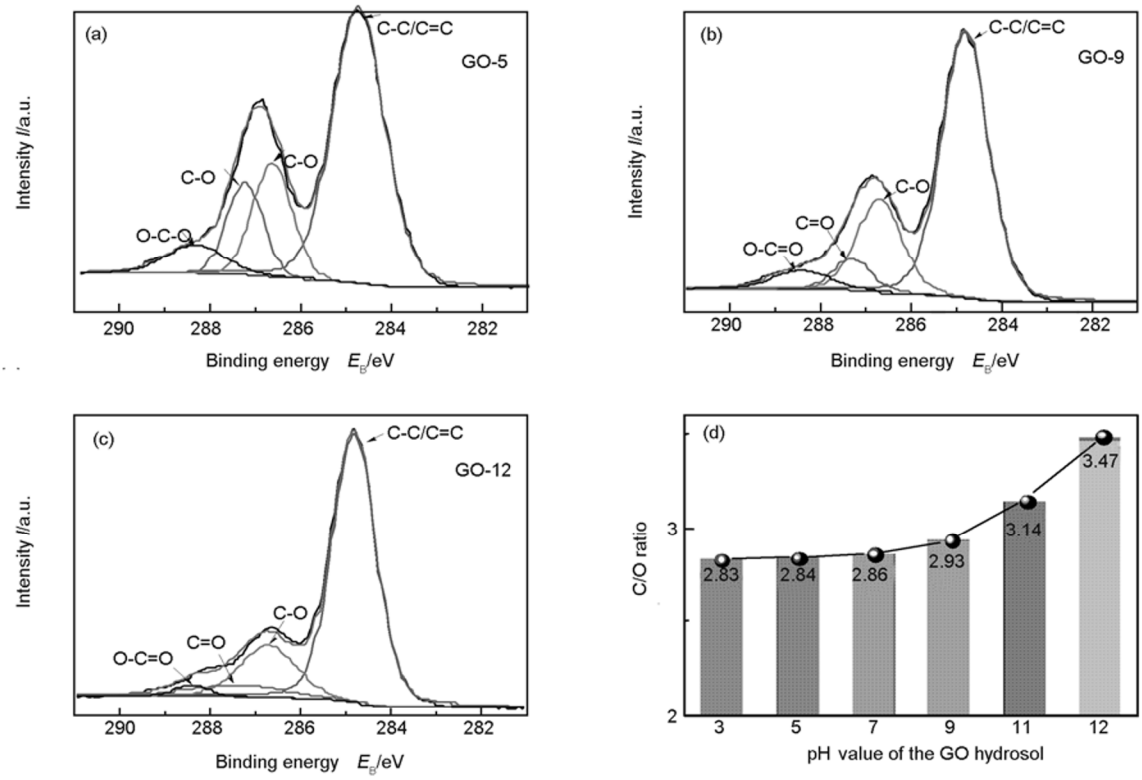

Fig. 2 pH-induced specific functionalization of GONs. The C1s profiles of GONs existed in the hydrosols of (a)GO-5, (b)GO-9 and (c)GO-12; (d)C/O ratio of the GONs.

of GO hydrosol into black. Detailed surface chemistry changes can be probed by XPS, and the results have been shown in Fig. 2d. In the pH values range of 3-7, the C/O ratio slightly increases, which could result from the size changes of the GONs, since small sheets have more functional groups fraction at the edge. And the increase of sheet sizes induces a slight increase of C/O ratio. On the contrary, the C/O ratio increases apparently with the pH value from 9 to 12 due to a serious removal of the oxygen-containing functional groups. The C1s profiles shown in Fig. 2a-c confirm the above discussion. The –C=O groups. The C_{1s} profiles shown in Fig. 2a-c confirm the above discussion. The –C=O and –O–C=O groups decrease apparently with the pH value from 5 to 9 compared with the C–O groups. After the pH value is tuned to 12, all above functional groups attached on GONs are removed obviously. Smaller sheet sizes of GONs will induce higher transmittances of GO hydrosol in acidic and neutral condition, and the removal of oxygen-containing functional groups and the retrieval of carbon aromatic ring may be the main factors that lead to the lower transmittance of GO hydrosol.

3.2 The electrochemical properties of GO hydrosol

The redox reaction in an aqueous ferrocyanide ($Fe(CN)_6^{4-}$) /ferricyanide ($Fe(CN)_6^{3-}$) system is a standard reaction in fundamental electrochemistry. Herein, we used this reaction to characterize the activity of the GONs with different surface chemistry and sheet sizes. Fig. 3a and b show the CV profiles of the GON modified GC electrodes in $K_3Fe(CN)_6$ electrolyte at the scan rate of 100 mV/s. The electrodes modified by the GO hydrosols with the pH values of 3, 5 and 7 all represent well-defined and sharp redox peaks and the peak-to-peak separation (ΔE_p) decreases slightly with the increase of the pH value. However, the ΔE_p shows a contrary change on the electrode modified by GONs in basic environment, which increases with increasing the pH value. The GO-12/GC and GO-11/GC represent the largest ΔE_p (174 and 180 mV) towards this reaction compared with those of others (55-75 mV). GO-7/GC and GO-9/GC exhibit a pair of stable, well-defined and nearly-symmetric reversible redox peaks with very low potential separation between anodic and cathodic peaks (The ΔE_p are 56 and 60 mV, respectively), indicating the rapid electron transfer rate and excellent electrochemical reversibility. Considering the ratios of the anodic current over the cathodic current, which are about 0.75 for GO-7/GC and 0.88 for GO-9/GC, GO-9/GC should possess a higher catalytic stability suggested by a more quasi-reversible redox process. The above results indicate that the large-size GONs have a higher activity since the GONs obtained in the hydrosols have similar surface chemistry in both acidic and neutral condition. It is found that the oxygen-containing functional groups play a very important role in promoting the electron transfer in the electrochemical catalytic process by comparing the properties of GO-5/GC

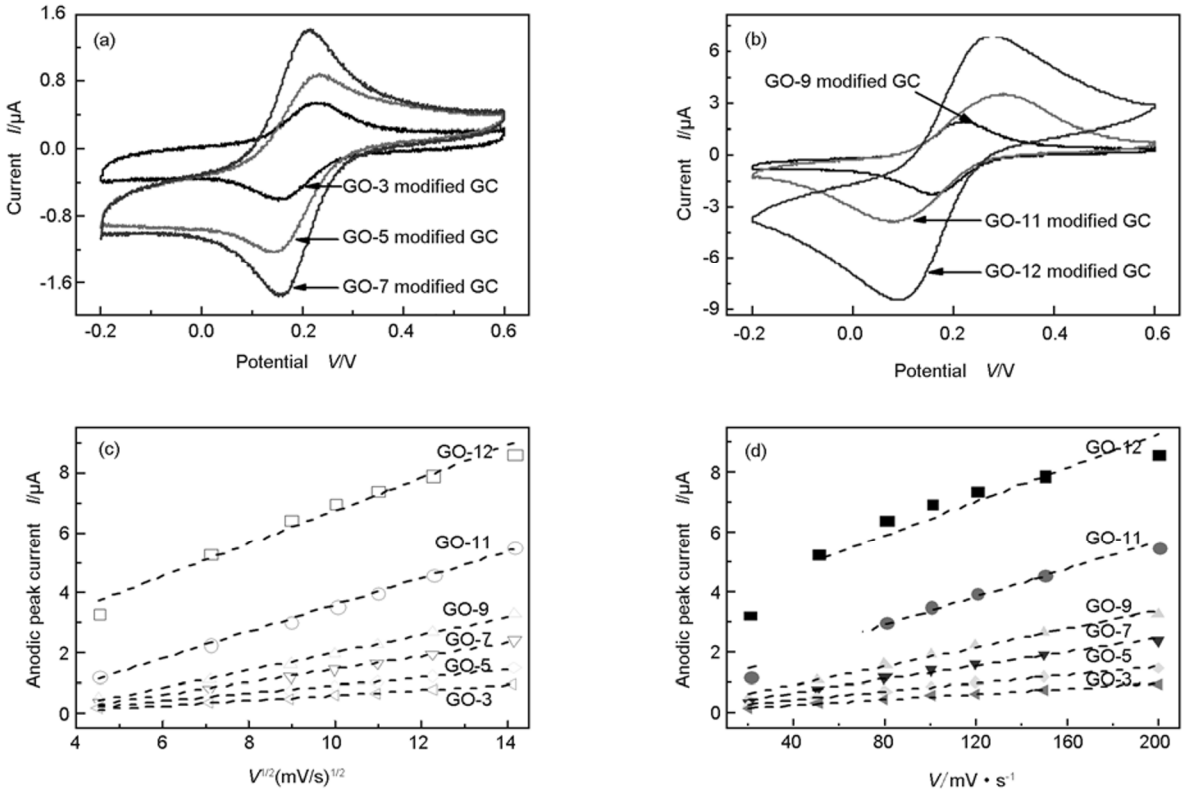

Fig. 3 Electrochemical behaviors of GO modified GC electrodes in ferricyanide electrolyte. (a) and (b) show the CV profiles of the modified GC electrodes with GO hydrosols at different pH values in 0.007 mol/L $K_3Fe(CN)_6$ at a scan rate of 100 mV/s; (c) and (d) show the plots of the anodic peak currents *vs.* $v^{1/2}$ and v, respectively (v denotes as scan rate).

with GO-11/GC, characterized by a similar sheet size. However, too many functional groups incorporated into GONs will induce the decrease of the electron transfer rate in the two-dimensional carbon network. From above discussion, we can find that the sheet size may be a key factor that affects the electrochemical activity of GONs revealed by a largely-enhanced electron transfer rate in the reaction, and the surface chemistry acts as another factor that promotes the electrochemical activity. These results also suggest that the carboxyl group is more active since it is the mostly removed group in strong basic conditions, and the detailed investigations are on-going now.

As shown in Fig. 3c and d, the anodic peak current increases with the increase of scan rates, and the linear relationships are found to exist between the anodic peak current (abbreviated as I_{pa}) and $v^{1/2}$ or v (v denotes the scan rate) for the electrodes modified with GO hydrosol. The oxidation peak current is linearly proportional to the scan rates, indicating a surface-confined electrochemical process for the redox reaction due to the limited conductivity of the GONs as we mentioned above, while the linear relationship between I_{pa} and $v^{1/2}$ indicates that this redox reaction is also a diffusion-controlled process since the diffusion transportation between the support electrolyte and the electrode surface during the reaction process is generally a slow process.

Fig. 4 shows the detailed CV curves of the electrodes at different scan rates, from which we can identify that the ΔE_p for all the electrodes obviously increase with the increase of the scan rates, especially for GO-11/GC and GO-12/GC. For most cases, large value of v induces the increase of the mass transfer coefficient, and thus the ΔE_p increase since a larger overpotential is needed to achieve the same rate of electron transfer. Although the GO-11/GC and GO-12/GC have a high conductivity which is reflected by the largely-increased peak current, the partial removal of the functional groups induces the decrease of the active sites, further leading to the restriction of electron transfer rate between the electrode and the reactant. By comparing the curves shown in Fig. 4, it is revealed that the GO-9/GC shows the highest catalytic stability, which is in correspondence with the aforementioned discussion. For the small sheets in the acidic condition, which have more active functional groups and edges, the destroy of the sp^2 carbon networks by the rational distributed sp^3 components also partly leads to the restriction of electron transfer rate from the electrode to the reactant, which may be the possible reason for the decrease of electron transfer rates in the reaction.

Based on the above discussion, the existence of the functional groups is the main factor that influences the electrochemical activity of the GONs. On one hand, they act as active sites of electrochemical reaction, but on the other hand, they restrict the electron transfer rate from the electrode to the reactant. As a result, a point should be found to balance the carbon network integrity and activive sites since either too many or too few functional groups on GONs limit the electron transfer rate.

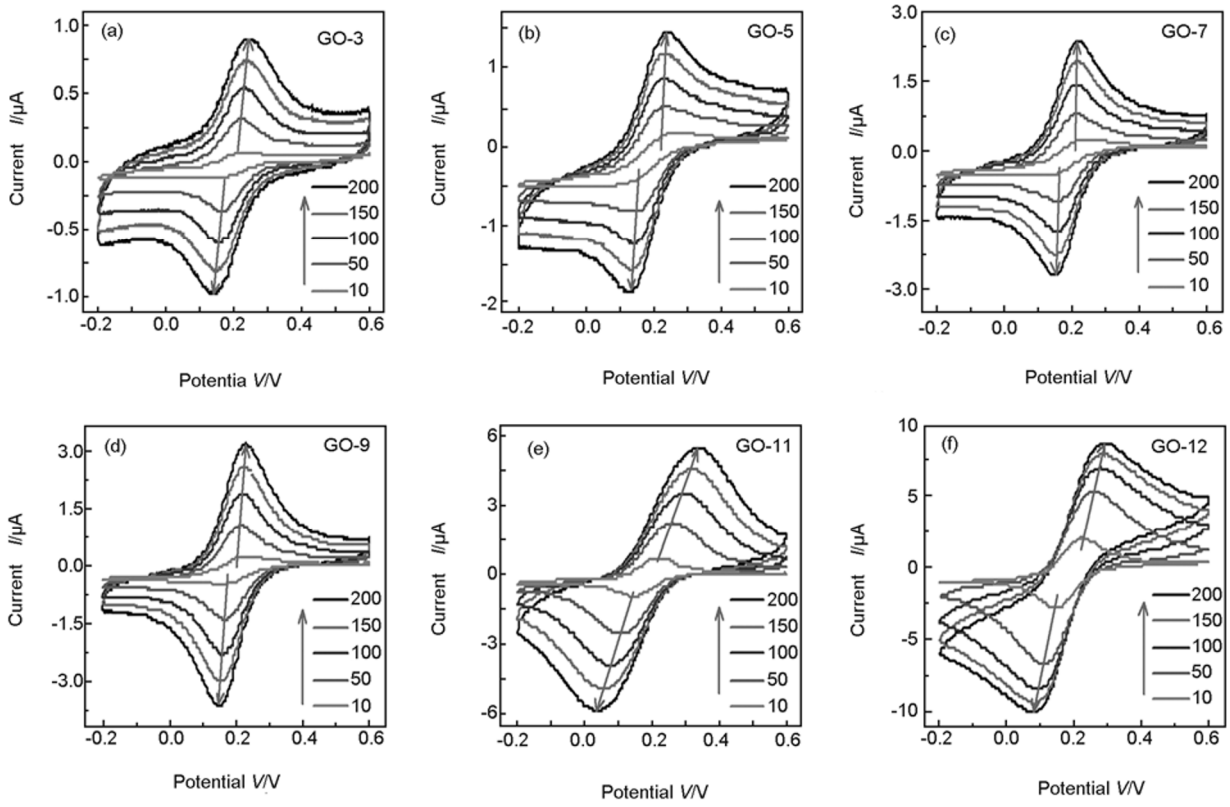

Fig. 4 CV profiles of GO modified GC electrodes in 0.007 mol/L $K_3Fe(CN)_6$ solution at different scan rates, and (a)-(f) show the detail information of GON in the hydrosols with the pH values of 3, 5, 7, 9, 11 and 12, respectively.

3.3 The electrochemical activity of GON towards H_2O_2 detection

In order to further explore the electrochemical activity of the GONs and the application prospect in electrochemical detection, we selected the electrodes with obvious differences as the typical examples and investigated their electrochemical behaviors towards the reduction of H_2O_2. As shown in Fig. 5a-c, obvious redox peaks can be observed in PBS buffered 0.1 mM H_2O_2 on the GONs modified electrodes, while the unmodified GC electrode shows no redox peaks. From the curves, no apparent difference is revealed, and the only obvious difference is that the peak current increases with the increase of the pH values of GO hydrosol. For GO-5/GC, an anodic peak also appeared in Fig. 5a, which may be derived from the electrochemical reduction of the functional groups on the GONs since it has a low C/O ratio. Fig. 5d shows the well-defined steady-state amperometric response of electrodes towards the successive addition of 0.3 mmol/L and then 1.5 mmol/L H_2O_2 at 0.6 V. The potential is selected according to the anodic peaks of the modified electrodes revealed in the CV curves. The response signals can be observed immediately after adding H_2O_2 and reach a steady-state level within 5 seconds, indicating a rapid and sensitive detection performance.

Compared with GO-12/GC, a more stable steady-state is achieved on the electrode of GO-5/GC and GO-9/GC after the H_2O_2 is added, indicating that a faster reaction is performed due to the fast electron transfer, which corresponds to the aforementioned discussions. Thus, they are more promising in a rapid quantitative detection. The electrodes show wide linear detection ranges (0.3-12 mmol/L) as shown in Fig. 5e. The current densities of GO-5/GC, GO-9/GC, GO-12/GC electrode and H_2O_2 concentrations display linear relationships with the sensitivities of 9.28, 22.02, 40.14 $\mu A \cdot mM^{-1} \cdot cm^{-2}$ and correlation coefficients of 0.992, 0.995, 0.998 respectively. The detection limits of GO-5/GC, GO-9/GC, GO-12/GC electrodes are 29.28, 62.16 and 68.28 μmol/L, respectively, which exhibit a comparable performance with those of previous reports[31,32], demonstrating a great potential of GONs in electrochemical application as sensors. Furthermore, the GONs used as the active materials are easy to operate in electrode preparation with a low cost, and the electrochemical properties of the GONs can be tuned by precisely controlling the pH value of the hydrosol, which provides a good applicability at different conditions. From this part of discussion, we found that although the electrochemical catalytic performance of the GONs in the strong basic condition is a little bit worse than that of the others, it shows the highest current density due to the partial reduction of

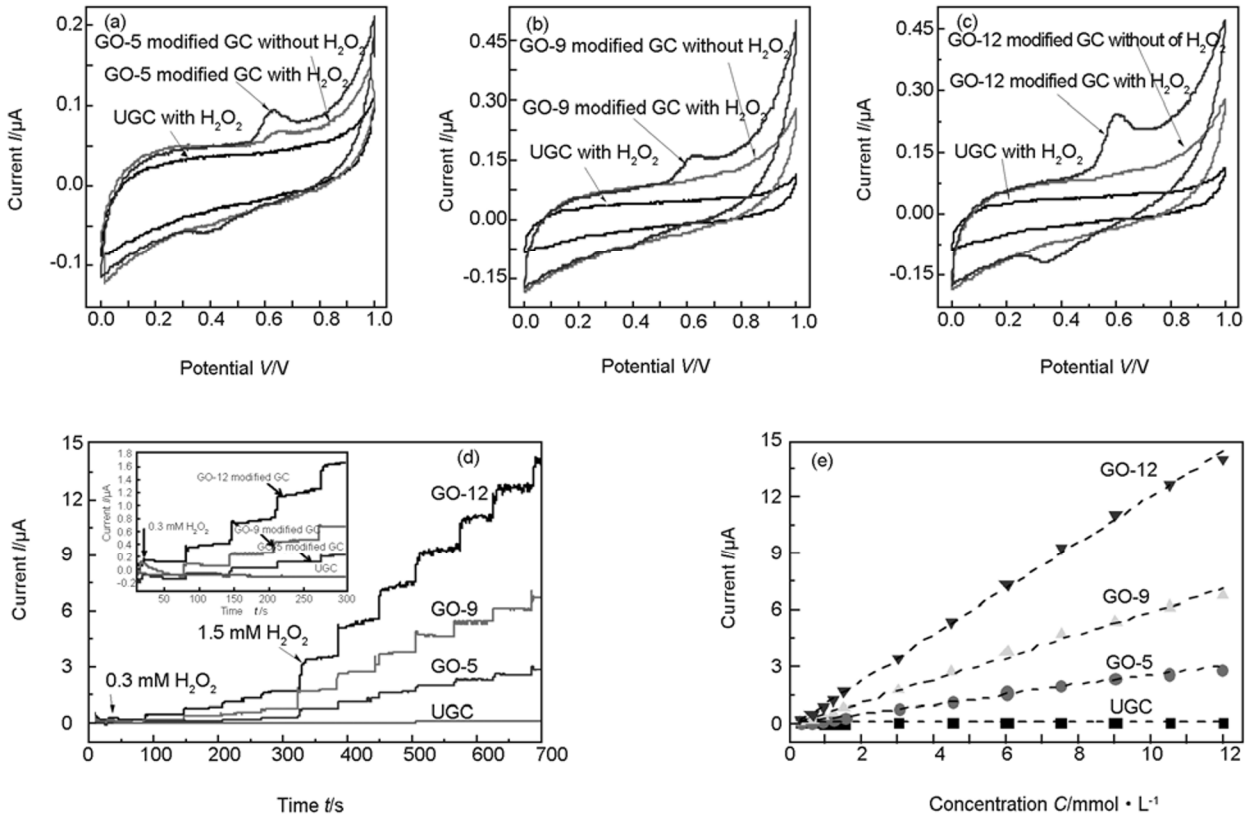

Fig. 5 Detection performance of the GO modified GC electrodes in 0.01 M PBS (pH=7.4). (a)-(c) show the CV profiles of (a) GO-5 , (b)GO-9 (c)and GO-12 modified GC electrodes in PBS without and with 0.1 mmol/L H_2O_2 respectively; (d) shows the detailed amperometric response of the GO modified electrode towards successive addition of H_2O_2 with gently stirring at 0.6 V, and (e) shows the plots of the corresponding current *vs.* the concentration of H_2O_2.

GONs, which decreases the demand for a high sensitive equipment. Thus, it also shows a great promising potential in the fast detection fields where a high precision is not needed.

4 Conclusions

In summary, the sizes and surface chemistry of GONs well dispersed in aqueous solution can be precisely tuned by adjusting the pH value of the parent GO hydrosol, which results in different chemical activities of the obtained GONs. Due to the protonation of carboxyl groups and the partial removal of oxygen-containing functional groups, the large GONs prefer to exist in the neutral and alkalescent environment while the small GONs tend to exist in the high or low pH value environment, and the surface chemistry makes slight change at acidic condition while the oxygen-containing functional groups are removed obviously at basic condition. Correspondingly, the GONs show a higher activity at acidic and neutral condition than at basic condition. The functional groups and the edges of the GONs can be viewed as active sites in electrochemical reaction, and the functional groups are proved to be more crucial to electrochemical activity than the edges since the GONs with similar sheet sizes and less groups show a weaker activity. But under the neutral and alkalescent condition, the GONs with smaller sheet sizes and richer functional groups show a weaker electron transfer activity in electrochemical reaction as compared to those with larger size and slightly less functional groups; that is to say, the size of GON is also a key factor to influence the chemical activity. Therefore, the fraction of the functional groups and sheet sizes should be compromised to obtain GONs with a high chemical activity. Besides, a high electrochemical activity of the GONs towards H_2O_2 detection is observed, which suggests a promising application of GONs as biosensors.

Acknowledgements

We appreciate the supports from National Natural Science Foundation of China (51072131); NSF of Tianjin, China (12JCZDJC27400); China Postdoctoral Science Foundation(2012M520012); State Key Laboratory of Heavy Oil Processing and Shenzhen Basic Research Project (JC201104210152A and JC201005270288A).

References

[1] Loh K P, Bao Q L, Ang P K, et al. The chemistry of graphene [J]. J Mater Chem, 2010, 20: 2277-2289.

[2] Dreyer D R, Park S, Bielawski C W, et al. The chemistry of graphene oxide [J]. Chem Soc Rev, 2010, 39: 228-240.

[3] Sarkar S, Bekyarova E, Haddon R C. Chemistry at the dirac point: diels-alder reactivity of graphene accounts [J]. Chem Res, 2012, 45(4): 673-682.

[4] Luo B, Liu S M and Zhi L J. Chemical approaches toward graphene-based nanomaterials and their applications in energy-related areas [J]. Small, 2012, 8(5): 630-646.

[5] ZHANG Li-fang ,WEI Wei, LU Wei, et al. Graphene-based macroform: preparation, properties and applications[J]. New Carbon Materials, 2013, 28(3): 161-171.

[6] Nardecchia S, Carriazo D, Ferrer M L, et al. Three dimensional macroporous architectures and aerogels built of carbon nanotubes and/or graphene: synthesis and applications [J]. Chem Soc Rev, 2013, 42: 794-830.

[7] Xu Y X, Sheng K X, Li C, et al. Self-assembled graphene hydrogel via a one-step hydrothermal process [J]. ACS Nano, 2010, 4(7): 4324-4330.

[8] Chen C M, Yang Q H, Yang Y G, et al. Self-assembled free-standing graphite oxide membrane [J]. Adv Mater, 2009, 21(29): 3007-30011.

[9] Lv W, Tao Y, Ni W, et al. One-pot self-assembly of three-dimensional graphene macroassemblies with porous core and layered shell [J]. J Mater Chem, 2011, 21: 12352-12357.

[10] Chen X C, Wei W, Lv W, et al. A graphene-based nanostructure with expanded ion transport channels for high rate Li-ion batteries [J]. Chem Commun, 2012, 48: 5904-5906.

[11] Lv W, Xia Z X, Wu S D, et al. Conductive graphene-based macroscopic membrane self-assembled at a liquid-air interface [J]. J Mater Chem, 2011, 21: 3359-3364.

[12] Zhu S J, Tang S J, Zhang J H, et al. Control the size and surface chemistry of graphene for the rising fluorescent materials [J]. Chem Commun, 2012, 48: 4527-4539.

[13] Zhang Y H, Zhou K G, Xie K F, et al. Tuning the electronic structure and transport properties of graphene by noncovalent functionalization: effects of organic donor, acceptor and metal atoms [J]. Nanotechnology, 2010, 21(6): 065201.

[14] Zhu Y W, Murali S, Cai W W, et al. Graphene and graphene oxide: synthesis, properties, and applications [J]. Adv Mater, 2010, 22(35): 3906-3924.

[15] Lv W, You C H, Wu S D, et al. pH-Mediated fine-tuning of optical properties of graphene oxide membranes [J]. Carbon, 2012, 50(9): 3233-3239.

[16] Bai H, Li C, Shi G Q. Functional composite materials based on chemically converted graphene [J]. Adv Mater, 2011, 23(9): 1089-1115.

[17] Bai H, Li C, Wang X L, et al. A pH-sensitive graphene oxide composite hydrogel[J]. Chem Commun, 2010, 46: 2376-2378.

[18] Zhao J P, Pei S F, Ren W C, et al. Efficient preparation of large-area graphene oxide sheets for transparent conductive films [J]. ACS Nano, 2010, 4(9): 5245-5252.

[19] Lin X Y, Shen X, Zheng Q B, et al. Fabrication of highly-aligned, conductive, and strong graphene papers using ultra large graphene oxide sheets [J]. ACS Nano, 2012, 6(12): 10708-10719.

[20] Yue H, Wei W, Yue Z G, et al. The role of the lateral dimension of graphene oxide in the regulation of cellular responses [J]. Biomaterials, 2012, 33(16): 4013-4021.

[21] Chen X M, Wu G H, Jiang Y Q, et al. Graphene and graphene-based nanomaterials: the promising materials for bright future of electroanalytical chemistry [J]. Analyst, 2011, 136(22): 4631-4640.

[22] Pumera M, Ambrosi A, Bonanni A, et al. Graphene for electrochemical sensing and biosensing [J]. Trac-Trend Anal

Chem, 2010, 29(9): 954-965.

[23] Han T H, Huang Y K, Tan A T L, et al. Steam etched porous graphene oxide network for chemical sensing [J]. J Am Chem Soc, 2011, 133(39): 15264-15267.

[24] Lv W, Guo M, Liang M H, et al. Graphene-DNA hybrids: self-assembly and electrochemical detection performance [J]. J Mater Chem, 2010, 20: 6668-6673.

[25] Lv W, Jin F M, Guo Q G, et al. DNA-dispersed graphene/NiO hybrid materials for highly sensitive non-enzymatic glucose sensor [J]. Electrochimica Acta, 2012, 73: 129-135.

[26] Pyun J. Graphene oxide as catalyst: application of carbon materials beyond nanotechnology [J]. Angew Chem Int Edit, 2011, 50(1): 46-48.

[27] Kim F, Cote L J, Huang J X. Graphene oxide: surface activity and two-dimensional assembly [J]. Adv Mater, 2010, 22(17): 1954-1958.

[28] Shih C J, Lin S C, Sharma R, et al. Understanding the pH-dependent behavior of graphene oxide aqueous solutions: a comparative experimental and molecular dynamics simulation study [J]. Langmuir, 2012, 28(1): 235-241.

[29] Wang X L, Bai H, Shi G Q. Size fractionation of graphene oxide sheets by pH-assisted selective sedimentation [J]. J Am Chem Soc, 2011, 133(16): 6338-6342.

[30] Fan X B, Peng W C, Li Y, et al. Deoxygenation of exfoliated graphite oxide under alkaline conditions: a green route to graphene preparation [J]. Adv Mater, 2008, 20(23): 4490-4493.

[31] Liu X, Xu X, Zhu H, et al. Synthesis of graphene nanosheets decorated with silver nanoparticles for enzymeless hydrogen peroxide detection[J]. Anal Methods, 2013, 5: 2298-2304.

[32] Ye Y, Kong T, Yu X, et al. Enhanced nonenzymatic hydrogen peroxide sensing with reduced graphene oxide/ferroferric oxide nanocomposites[J]. Talanta, 2012, 89: 417-421.